Behavior during quenches of a 40 T magnet made of LTS and HTS parts

Philippe Fazilleau, Simon Bagnis, Matthias Durochat, Thibault Lécrevisse, Clément Lorin, Xavier Chaud, Andrew Varney, Steven Ball, Roman Viznichenko and Andrew Twin

***Abstract*—In the framework of the SuperEMFL (Super European Magnetic Field Labs) project, we have previously studied numerous possible pre-designs made of an HTS insert with a LTS outsert to achieve a central magnetic induction of 32 T and 40 T. From the most interesting designs, the behavior of the magnet has been studied during the quench of one of the superconducting parts, either LTS or HTS one. This study includes a multi-physics analysis (magnetics, thermics, mechanics) of both parts and has been led with two different codes, each one based on a very different protection principle. We showed that the quench of the LTS outsert, as it is adequately protected, caused a quasi-symmetrical quench of the HTS part, with a limited increase of the temperature. However, the ignition of the quench within the HTS insert leads to an asymmetrical current distribution and to a significant axial force resultant generated on the LTS part. This may necessitate mechanical reinforcement to address the resulting imbalance.**

I. Introduction

THIS article presents a comprehensive exploration of the dynamic behavior exhibited by high-field superconducting magnets comprising both Low-Temperature Superconductors (LTS) and High-Temperature Superconductors (HTS) parts. The investigation is situated within the ambit of the SuperEMFL European project, which seeks to advance the capabilities of high-field magnet technology. The study specifically focuses on understanding the intricate dynamics of the HTS and LTS parts during quench events.

Several superconducting magnets recently generate 32 T [1] or more [2]. The NOUGAT (Nouvelle Generation d'Aimant supraconducteur pour la production de Teslas) HTS insert [3], was validated through testing in resistive coils up to 32.5 T and has paved the way for deeper investigations. This research delves into hybrid 32 T and 40 T designs, made of HTS and LTS parts, aiming at illuminating the magnet's response under quench events.

The investigation is multifaceted, encompassing magnetic, thermal, and mechanical aspects. Some authors have already studied the quench of insulated HTS windings [4]. The novelty consists in the study of the quench of an HTS MI winding subjected to the constraints of an external LTS winding. The key goals of this study are twofold: (1) to analyze the thermal responses of both LTS and HTS coils when subjected to quench events and (2) to quantitatively evaluate the forces generated within each superconducting part during diverse quench scenarios. Understanding these dynamics is essential not only for ensuring the safe operation of superconducting magnet systems but also for enhancing their performance and reliability.

The remainder of this article is structured as follows. Section II outlines the methodologies employed for modeling quench dynamics and introduces the protection principles used in each part of the hybrid magnet. Section III provides a detailed description of the superconducting parts and their electrical circuitry. Section IV presents the results of the quench simulations, discussing both LTS and HTS quench scenarios.

Philippe Fazilleau, Simon Bagnis, Matthias Durochat, Thibault Lécrevisse, Clément Lorin are with Université Paris-Saclay, CEA, Department of Accelerators, Cryogenics, and Magnetism, 91191, Gif-sur-Yvette, France. Xavier Chaud is with LNCMI-EMFL, CNRS UPR3228, Univ. Grenoble Alpes, France. Andrew Varney, Steven Ball, Roman Viznichenko and Andrew Twin are with Oxford Instruments Nanoscience, Abingdon-on-Thames, United Kingdom.

II. Modeling of the Quench

In this section, we delve into the protection principles employed in both the HTS and LTS parts, shedding light on the respective modeling codes used.

A. 3D Propagation Modeling of the LTS Coils

Quench dynamics within LTS coils are conventionally simulated by employing 3D propagation velocities coupled with homogenized material properties. This approach finds its basis in the work of Wilson [5], particularly tailored for the modeling of insulated LTS windings.

B. Partial Element Equivalent Circuit (PEEC) Modeling for HTS Coils

When it comes to Metal-as-Insulation (MI) [6], [7] or No Insulation (NI) windings, a paradigm shift occurs due to the distinct nature of current flow, allowing radial currents to be present.

To account for the specific characteristics of HTS coils, we have developed several computational codes in MATLAB [8] capable of accounting for the nuanced electric circuitry., based on the Partial Element Equivalent Circuit (PEEC) model [9], [10].

However, the computational demands are substantial due to the expansive number of elements required. Moreover, the inherently nonlinear Ordinary Differential Equations (ODEs), replete with full matrices, particularly for magnetic coupling, amplify computational complexity. These equations need to be solved at each time step, a task demanding extensive computation time.

To address these computational challenges, we have developed two specialized PEEC codes, aimed at streamlining

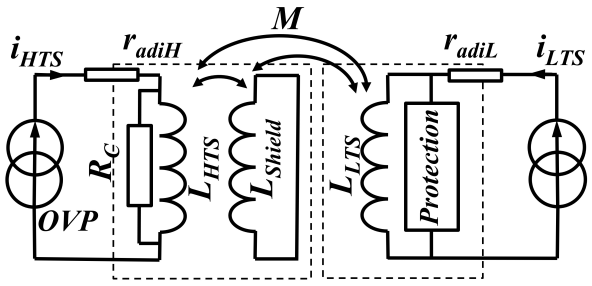

Fig. 1. Schematic representation of the electrical circuit of the coupled LTS and HTS parts. See below for definitions of the elements.

the modeling process. For magnets consisting of a single coil, we have introduced the PEEC-S (Simplified) code. Here, each element corresponds to one or multiple turns, facilitating axisymmetrical representation of the quench dynamics.

III. Description of the Superconducting Parts

In ensuring the safe operation of a coupled LTS-HTS magnet, it is imperative to assess the quench dynamics and temperature rise within each constituent part of the magnet.

The simplified electrical circuitry is depicted in Figure 1, illustrating the magnetic coupling between the LTS and HTS parts. Notably, each part of the magnet is endowed with its own dedicated power supply, functioning in tandem with the magnetically coupled circuitry.

Several parameters are essential to the circuit description:

- R_c represents the turn-to-turn contact resistance of 10 $mOhm.cm^2$ resistivity. This value has been set as it fits well with experiments of prototypes made of MI windings [11].
- r_{adiH} and r_{adiL} denote the resistances of the cables and current leads between each magnet part and their respective power supply.
- L_{HTS} and L_{LTS} represent respectively the inductance matrix of the HTS and LTS winding.
- L_{shield} denotes the inductance matrix of the HTS shielding.
- M symbolizes the total mutual inductance matrix between all the inductances (L_{HTS}, L_{LTS}, L_{shield}).

The HTS shielding is performed with several short-circuited turns of No-Insulation (NI) winding at the external radius of each pancake. Of paramount importance, the HTS coil's power supply encompasses an Over Voltage Protection (OVP) mechanism. This feature comes into play when the voltage across its terminals reaches the pre-defined OVP value. Consequently, the current initiates a decrement in order to maintain a constant voltage value. By judiciously selecting an appropriate OVP threshold – set to 5 V in the quench calculations – an additional passive protection feature is incorporated into the system.

A. Quench Initiated within the LTS Outsert Magnet

The LTS outsert is a magnet sourced from Oxford Instruments NanoScience [12]. Characterized by 6 nested coils, the LTS magnet's protection circuitry is primarily passive in nature. Key elements include diodes designed to divert current flow within quenched zones and activate heaters to propagate normal zones [13], labelled as Protection in Figure 1.

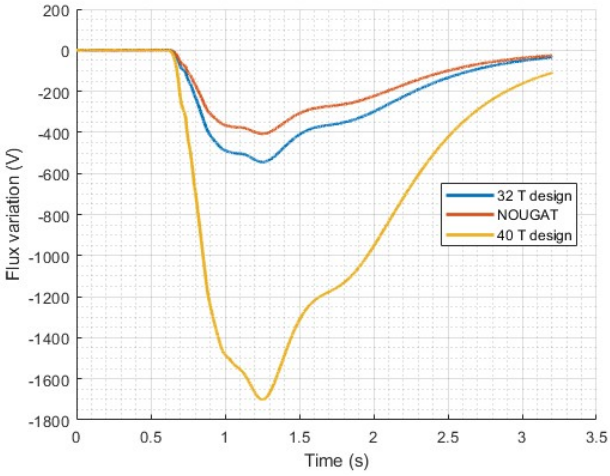

Fig. 2. Magnetic flux variation at the terminals of the HTS part during a quench of the LTS part.

TABLE I
PARAMETERS OF HTS PARTS.

	NOUGAT 32 T	SEMFL 32 T	SEMFL 40 T
Tape	SUPERPOWER	THEVA APC	THEVA APC
Double-pancakes	9	8	25
Turns per pancake	290	360	360
Nominal current	281 A	336 A	310 A
Critical current	304 A	472 A	397 A
Current margin	8 %	29 %	22 %
Self-Inductance	0.846 H	1.244 H	10.93 H
Winding Inner radius	25 mm	25 mm	25 mm

Figure 2 shows the flux variation at the terminals of the HTS part during a quench of the LTS part [14]. With inductance values from 1 to 10 H, the current ramp-rates can reach values up to 300 A/s.

B. Quench Initiated within the HTS Insert Magnet

The self-protective feature of the NI/MI windings has been employed in the HTS insert and is complemented with OVP principle and shielding protection to mitigate external magnetic flux variations.

Importantly, the quench propagation within HTS magnets deviates from LTS behavior, lacking axial symmetry. The ignition of a quench within the HTS magnet primarily occurs in the upper internal radius zone, in liquid helium (LHe) bath cooling. The magneto-gravitational forces induced by the high magnetic field gradient in the helium coolant provoke the entrapment of helium bubbles, undermining cooling efficiency and, consequently, potentially leading to quench events. [15], [16].

In computational simulations, quench events are deliberately triggered in proximity to these zones. Our analysis encompasses three distinct HTS magnets, each detailed in Table I.

The designs considered include the NOUGAT magnet [3] in a 32 T hybrid configuration (13 T from the insert alone

This article has been accepted for publication in IEEE Transactions on Applied Superconductivity. This is the author's version which has not been fully edited and content may change prior to final publication. Citation information: DOI 10.1109/TASC.2024.3370138

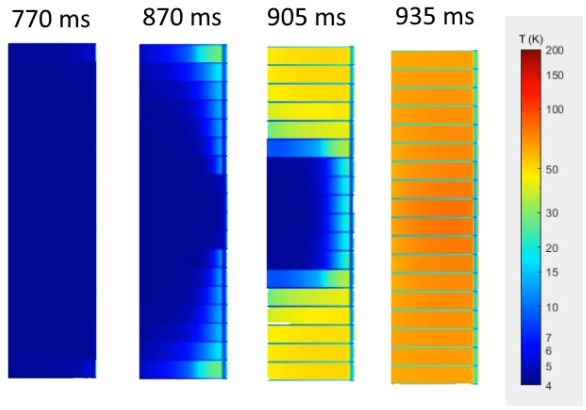

Fig. 3. Evolution of the temperature within the cross-section of the NOUGAT magnet during a quench of the LTS part triggered at t = 0 s.

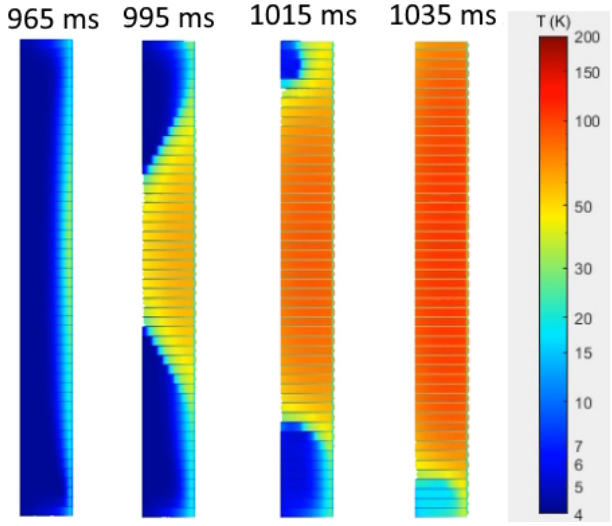

Fig. 4. Evolution of the temperature within the cross-section of the HTS insert of the SEMFL 40 T magnet during a quench of the LTS part triggered at t = 0 s.

and 19 T from a LTS outsert), the SuperEMFL 32 T baseline design from the initial project phase [17], and a SuperEMFL single coil 40 T design [18].

IV. Quench: Results and Discussion

A. Quench of the LTS Outsert

As previously mentioned, a quench initiated in the LTS outsert exhibits quasi-complete axial symmetry, leading to a quasi-symmetrical quench in the HTS insert.

Figure 3 displays the temperature distribution of the HTS magnet, specifically the NOUGAT design, at different time intervals during a quench triggered by the magnetic flux variation from the quenched LTS magnet. The temperature distribution is entirely symmetrical with respect to the mid-plane. Likewise, the radial and azimuthal current distributions are symmetrical. The quench propagates radially and axially due to the turn-to-turn thermal conductivity and is driven by the joule losses of the radial currents.

For this design, the total Lorentz force resultant generated within each superconducting part is null. The radial component is null due to the problem's axisymmetry, while the axial component is null due to the axial symmetry of both the quench and azimuthal current distribution.

However, due to the anisotropy of THEVA Artificial Pinning Conductor (APC) which shows a deviation of 30° between the (ab) plane and the tape plane, the quench ignition is not completely symmetrical in the axial direction for SuperEMFL designs if pancakes are wound with the same tape orientation in all the pancakes. The differing critical current symmetry leads to this behavior. Figure 4 illustrates the evolution over time of the temperature distribution within the pancakes of the 40 T SuperEMFL design.

This asymmetrical distribution results in a non-axial component of the resultant Lorentz force within the LTS coil. The resultant forces in the LTS part, with respect to time, are shown (plain lines) for the three designs in Figure 5. The axial resultant force can reach more than 20 tons for the case of the 40 T design with the THEVA APC. This could be easily solved by reversing the tape in one of the halves of the magnet.

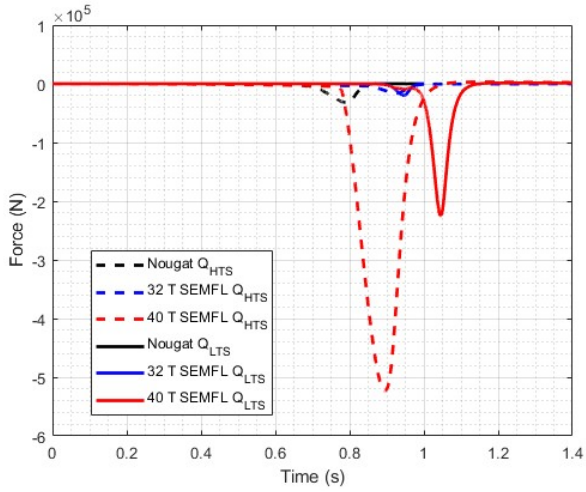

Fig. 5. Evolution of the axial resultant force within the LTS part during a quench. The solid lines show the cases of a quench ignited in the LTS part, generating a quench of the HTS part, labelled as Q_{LTS}. The dash lines show the cases of a quench ignited in the HTS part, labelled as Q_{HTS}.

Figure 6 illustrates the evolution of the maximal temperature of the HTS part over time (solid lines) for the three designs listed in Table I. Across all designs, the maximal temperature remains below 120 K, a sufficiently low temperature to avoid endangering the HTS magnet.

B. Quench of the HTS Insert

As observed in the preceding section, quench ignition in the HTS outsert primarily occurs in the upper internal region of the magnet.

Figure 7 displays the evolution of temperature distribution in the case of the NOUGAT magnet. Notably, the distribution is not symmetrical.

Whatever the design, the quench propagation follows a two-step pattern: first, the quench expands from the ignition

This article has been accepted for publication in IEEE Transactions on Applied Superconductivity. This is the author's version which has not been fully edited and content may change prior to final publication. Citation information: DOI 10.1109/TASC.2024.3370138

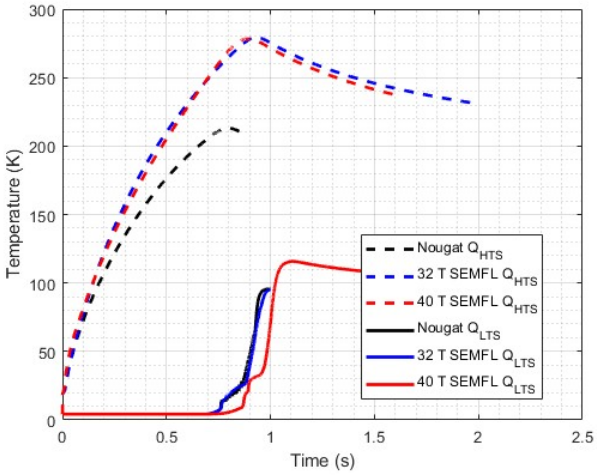

Fig. 6. Evolution of the maximal temperature within the HTS part during a quench. The solid lines show the cases of a quench ignited in the LTS part, generating a quench of the HTS part, labelled as Q_{LTS}. The dash lines show the cases of a quench ignited in the HTS part, labelled as Q_{HTS}.

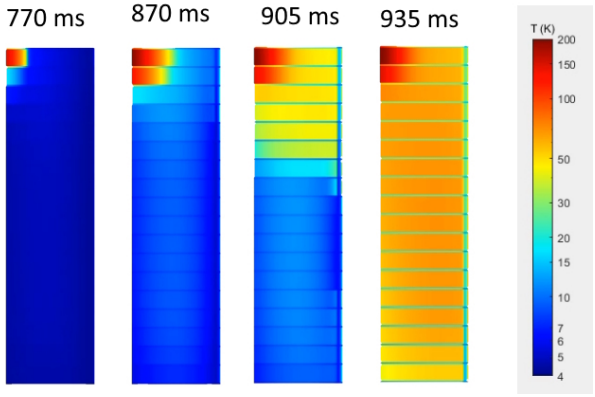

Fig. 7. Evolution of the temperature within the cross-section of the NOUGAT magnet during a quench of the HTS part.

point, accompanied by an increase in temperature. Second, a rapid and complete quench propagation throughout the entire magnet occurs in less than 200 ms. Figure 8 demonstrates this pattern with the evolutions of the maximal current within the winding during a quench of the HTS part. The complete propagation to the whole winding appears during the peak zone, just before the fast decrease of the current. The duration of the initial phase primarily hinges on the current margin, with the SuperEMFL designs exhibiting longer initial phases due to their higher current margins.

Maximal temperature evolutions over time for the three designs listed in Table I are depicted in Figure 6 (dash lines). Maximal temperatures are below 300 K, a level achieved due to the self-protective feature of MI windings and the Over Voltage Protection (OVP) mechanism in the power supply.

The evolutions with time of the axial resultants of the Lorentz force generated in the LTS magnet are shown in Figure 5 (dash lines). The magnitude of the axial force resultant can be substantial, up to 50 tons in the case of the 40 T SEMFL design, making compulsory a mechanical reinforcement for the

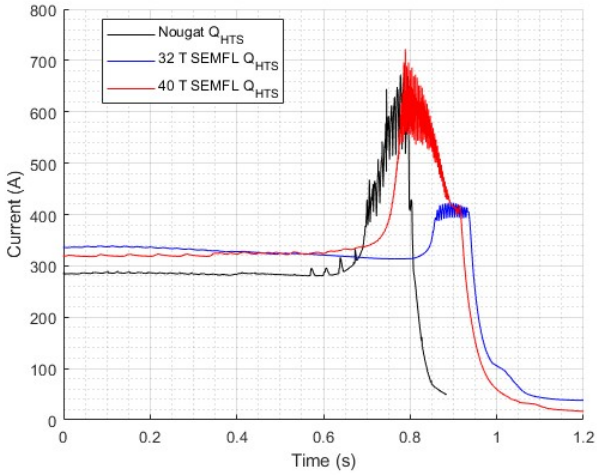

Fig. 8. Evolution of the maximal current within the HTS winding during a quench of the HTS part. The LTS part remains superconducting and its magnetic field constant.

19 T magnet to withstand these forces. Moreover, the stresses generated within the HTS insert could be very high due to the overcurrent and consequently could damage the winding. This mechanical issue is actually under study.

V. Conclusion

Our study has effectively addressed key objectives related to the dynamic behavior of high-field superconducting magnets comprising both LTS and HTS components. We successfully addressed the primary objectives of our research, which included a thorough analysis of the thermal responses exhibited by LTS and HTS coils during quench events, as well as a quantitative assessment of the global forces generated within the system.

The thermal analysis has provided compelling evidence for the feasibility and safety of the proposed magnet designs. The recorded maximum temperatures during quenches remained well below established safety thresholds.

Furthermore, the mechanical analysis has revealed a crucial insight: the occurrence of a quench in the HTS portion can give rise to exceptionally potent axial forces within the LTS part. This phenomenon underscores the imperative need for mechanical reinforcement measures to safeguard the structural integrity of the system.

Acknowledgments

The SuperEMFL project received funding from the European Union's Horizon 2020 research and innovation program under grant agreement No 951714. Any dissemination of results reflects only the author's view and the European Commission is not responsible for any use that may be made of the information it contains.

References

[1] H. W. Weijers, W. D. Markiewicz, A. V. Gavrilin, A. J. Voran, Y. L. Viouchkov, S. R. Gundlach, P. D. Noyes, D. V. Abraimov, H. Bai, S. T. Hannahs, and T. P. Murphy, "Progress in the development and construction of a 32-t superconducting magnet," *IEEE Transactions on Applied Superconductivity*, vol. 26, no. 4, pp. 1–7, 2016.

[2] J. Liu, Q. Wang, L. Qin, B. Zhou, K. Wang, Y. Wang, L. Wang, Z. Zhang, Y. Dai, H. Liu, X. Hu, H. Wang, C. Cui, D. Wang, H. Wang, J. Sun, W. Sun, and L. Xiong, "World record 32.35 tesla direct-current magnetic field generated with an all-superconducting magnet," *Superconductor Science and Technology*, vol. 33, no. 3, p. 03LT01, feb 2020. [Online]. Available: https://dx.doi.org/10.1088/1361-6668/ab714e

[3] P. Fazilleau, X. Chaud, F. Debray, T. Lécrevisse, and J.-B. Song, "38 mm diameter cold bore metal-as-insulation hts insert reached 32.5 t in a background magnetic field generated by resistive magnet," *Cryogenics*, vol. 106, p. 103053, 2020.

[4] L. Cavallucci, M. Breschi, P. L. Ribani, A. V. Gavrilin, H. W. Weijers, and P. D. Noyes, "A numerical study of quench in the nhmfl 32 t magnet," *IEEE Transactions on Applied Superconductivity*, vol. 29, no. 5, pp. 1–5, 2019.

[5] M. N. Wilson, *Superconducting Magnets*. Oxford University Press, 1983.

[6] R. Bailey *et al.*, "Metallic insulation for superconducting coils," Patent US4 760 365A, 1988.

[7] T. Lécrevisse, X. Chaud, P. Fazilleau, C. Genot, and J.-b. Song, "Metal-as-insulation hts coils," *Superconductor Science and Technology*, 2022. [Online]. Available: http://iopscience.iop.org/article/10.1088/1361-6668/ac49a5

[8] T. M. Inc., "Matlab version: 9.13.0 (r2022b)," Natick, Massachusetts, United States, 2022. [Online]. Available: https://www.mathworks.com

[9] T. Wang, S. Noguchi *et al.*, "Analyses of transient behaviors of no-insulation rebco pancake coils during sudden discharge and overcurrent," *IEEE Transactions on Applied Superconductivity*, vol. 25, p. 4603409, 2015.

[10] C. Genot, T. Lecrevisse, P. Fazilleau, and P. Tixador, "Transient behavior of a rebco no-insulation or metal-as-insulation multi-pancake coil using a partial element equivalent circuit model." *IEEE Transactions on Applied Superconductivity*, pp. 1–1, 2022.

[11] C. Genot, T. Lécrevisse, P. Fazilleau, and P. Tixador, "Experimental measurements of contact resistivity between superconducting hts tapes with or without metallic cowound tape," *Cryogenics*, vol. 132, 2023.

[12] Nanotechnology Now. (2014) Nanotechnology now - press release: "super power achieves 32.8

[13] D. Warren, A. Twin, Z. Melhem, P. Noonan, and M. Lakrimi, "GB2512372B," Patent, 2014.

[14] A. Varney, P. Fazilleau, S. Ball, R. Viznichenko, E. Pardo, A. Twin, X. Chaud, N. Jerance, T. Lécrevisse, and A. Dadhich, "Modelling and design implications of quenches in hybrid hts/lts high field magnets," 2023, poster presentation at MT28, to be published.

[15] W. D. Markiewicz, H. W. Weijers, P. D. Noyes, U. P. Trociewitz, K. W. Pickard, W. R. Sheppard, J. J. Jaroszynski, A. Xu, D. C. Larbalestier, and D. W. Hazelton, "33.8 TESLA WITH A YBa2Cu3O7x SUPERCONDUCTING TEST COIL," *AIP Conference Proceedings*, vol. 1218, no. 1, pp. 225–230, 04 2010. [Online]. Available: https://doi.org/10.1063/1.3422357

[16] D. Jiang, Y. Tan, G. Zou, X. Qian, S. Jiang, Z. Chen, W. Chen, and G. Kuang, "Energizing behaviors of a no-insulation and layer-wound rebco coil in high magnetic field," *Cryogenics*, vol. 101, pp. 1–6, 2019. [Online]. Available: https://www.sciencedirect.com/science/article/pii/S0011227518303096

[17] P. Fazilleau, X. Chaud, and T. Lécrevisse, "Superemfl project 32 t+ magnetic pre-designs," SuperEMFL project, Tech. Rep., July 2022.

[18] M. Durochat and P. Fazilleau, "Superemfl project 40 t+ magnetic pre-designs," SuperEMFL, Tech. Rep., August 2023.